Fizika Nizkikh Temperatur 1996, v. 22, No 2, p. 218–221

Phase diagrams of Ar–Xe, Kr–Xe, and Kr–CO binary alloys

L. D. Yantsevich, A. I. Prokhvatilov, and A. S. Barylnik

B. Verkin Institute for Low Temperature Physics and Engineering, National Academy of Sciences of Ukraine, 47, Lenin Ave., 310164, Kharkov, Ukraine
E-mail:brodyanskii@ilt.kharkov.ua

Using the powder x-ray diffraction method, the phase diagrams of the binary systems Ar–Xe, Kr–Xe, and Kr–CO have been studied. The molar volumes of these solutions versus temperature and composition have been determined within the homogeneity regions. A considerable deviation of the solubility from the Hume-Rosery rules (which is valid for metal alloys) has been found.

Atomic and molecular impurities in cryocrystals make it possible to change substantially many of their properties such as lattice dynamics, phase transitions, phase stability, etc. Therefore, of considerable interest is to study the $T-x$ phase diagrams of various binary cryocrystal systems. Mutual solubility of the components and the shape of the phase diagrams are to a large extent controlled by the difference in their molecular parameters (σ and ε) and in the nature of the interaction between the particles.

In this report we studied the phase diagrams of three binary systems, Ar–Xe, Kr–Xe, and Kr–CO. The atom-atom interactions of the constituent components in the Ar–Xe and Kr–Xe systems can be described by a Lennard-Jones-type potential, whereas the difference of the σ parameters amounts to 13 and 8%, respectively. In the CO–Kr system the difference in σ is small (4%), but the interaction between CO molecules is noticeably anisotropic due to the large quadrupole moment of the CO molecule [1]. According to the Hume-Rosery rules [2], at least for the last two systems one could expected unrestricted mutual solubility. At the same time, as established in vapor pressure measurements by Heastie and Lefebvre [3], the Ar–Xe system exhibits an eutectic point at $T = (82.3 \pm 0.6)$ K and an Ar concentration of (23.5 ± 0.5)%.

As was established in electron diffraction studies of Kovalenko et al. [4] on quench-condensed Xe–Ar films of thickness 80–200 Å, a wide region of separation exists at low temperatures. The solubility of xenon in argon for thin films turned out to be much higher then expected from the equilibrium phase diagram [3].

For the Kr–Xe system, Heastie has shown [5] that the liquidus and solidus have points of equal concentrations at a temperature of 114.1 K and a xenon concentrations of 15%, which also does not rule out a possibility of the solution to separate in the solid state. This conclusion is in line with the previously evaluated critical separation temperature of Freeman and Halsey [6], which was 92 K specifically for the Kr–Xe solutions. At the same time, electron diffraction studies of Kr–Xe condensates of thickness from 10 to 100 Å in the range of Kr fractions from 10 to 90% and temperatures 6 to 45 K [4] did not reveal any indication of the separation.

The melting diagram of the Kr–CO system is unknown. Solubility in the solid was studied by electron diffraction by Kovalenko et al. [7], who found that in the region of intermediate concentrations a phase separation of thin-film Kr–CO samples occurs at low temperatures. They observed amorphous states when the mixtures of compositions with more than 40% CO were quench condensed on $T = 2.3$ K. These film recrystallized, forming hcp crystals, when warmed up above 15 K.

Experimental

The studies were carried out using the x-ray diffraction method at temperatures from 6 K to the melting temperatures of the mixtures in the range of Kr and Xe concentrations from 2 to 99% on polycrystal samples, the purity of the source components being 99.99%.

The samples of solid solutions were prepared by condensation of gas mixtures of preset concentrations on a substrate cooled to a temperature of 40 K for the Ar–Xe and Kr–CO systems and 60 K for the Kr–Xe system. The samples were annealed at a temperature 10 to 30 K higher than the deposition temperature during 30–40 min. The position of the boundaries of the phase diagrams were determined from the structure of the phases and from lattice parameters as functions of temperature and composition. The accuracy of the lattice parameter determination in the mixtures was ± 0.04%. The phase boundaries and the points of three-phase equilibrium were on the average determined with an accuracy of ± 2% in concentration and ± 1 K in temperature.

Results

The phase diagrams thus obtained are shown in Figs. 1–3. The Ar–Xe and Kr–Xe systems exhibit a phase separation in the solid in a wide range of temperatures and compositions. The difference is that in the latter case the separation occurs not as a result of an eutectic reaction, as is the case for the Ar–Xe system, but below a critical concentration point with $T_{cr} = (75 \pm 2)$ K. The exact concentration position of the critical point has not been established owing to the broad flat crest of the separation curve. The difference of the fcc_{Xe} and fcc_{Kr} phase in the Kr–Xe system is likely to be due to the amount and character of the inhomogeneous strain displacements in the krypton-based and xenon-based solutions. In both systems the solubility below 50 K is low, reaching (3 ± 1)% of krypton in xenon and (4 ± 1)% of xenon in krypton for the Kr–Xe system and, for the

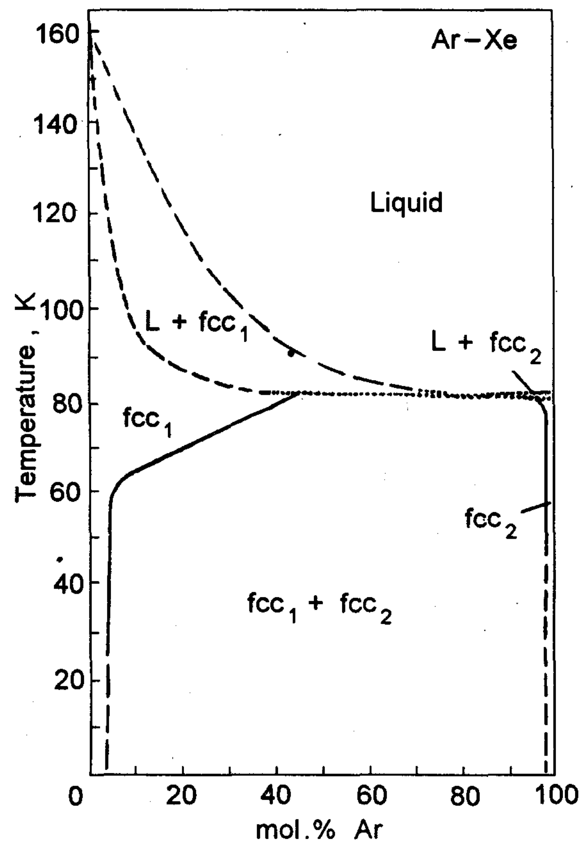

Fig. 1. Phase diagram of Ar–Xe mixtures: data of this work (———); tentative position of the solidus-liquidus curve (– – –); from Heastie and Lefebvre [3] (· · · ·).

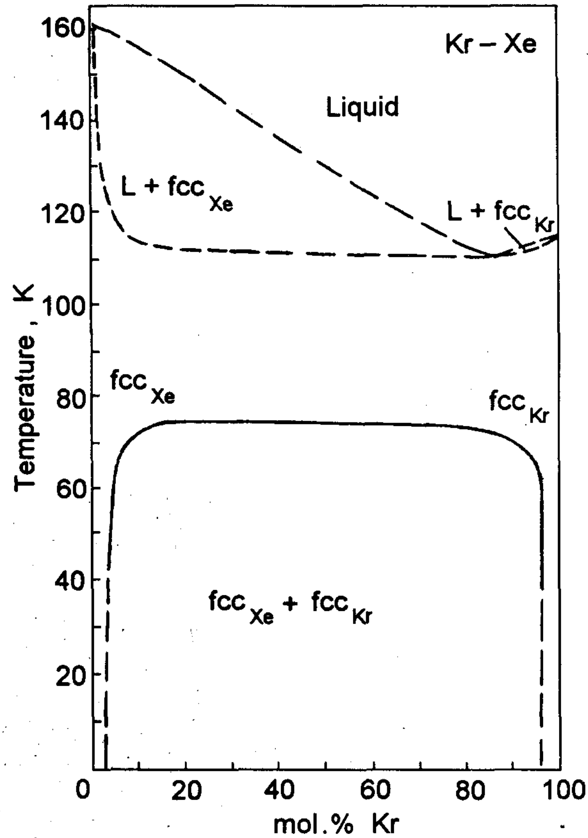

Fig. 2. Phase diagram of Kr–Xe mixtures: data of this work (———); hypothetic position of the equilibrium lines (– – –).

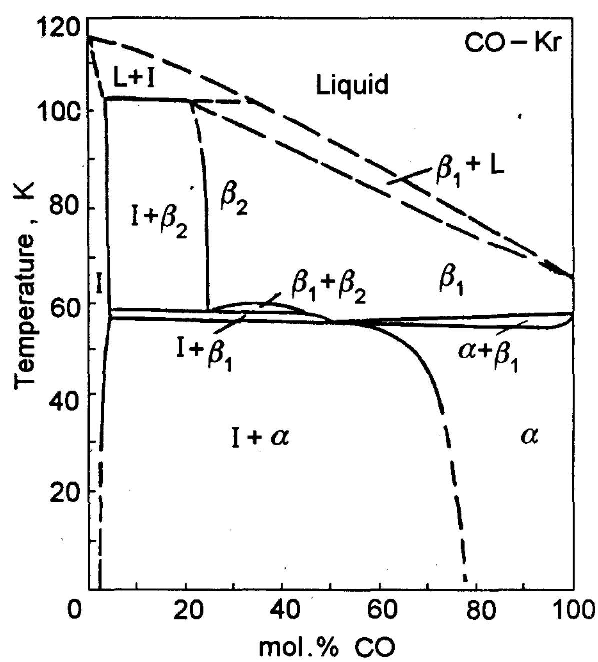

Fig. 3. Phase diagram of Kr–CO mixtures: data of this work (———); hypothetic position of the equilibrium lines (– – –).

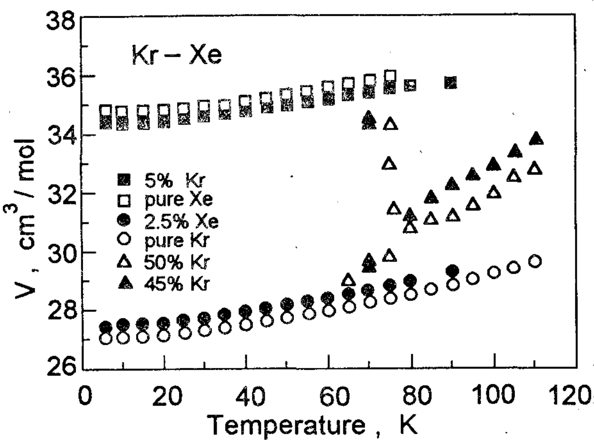

Fig. 4. Temperature dependence of the molar volume of Kr–Xe solutions.

Ar–Xe system, $(4 \pm 1)\%$ of argon in xenon and $(2-3) \pm 1\%$ of xenon in argon. At higher temperatures the solubility increases fast to reach 45% of xenon in argon at the eutectic point for the Ar–Xe system. By contrast, the solubility of argon in xenon is almost constant within the whole range of existence of solid solutions. Our data for the high-temperature region agree well with those of Heastie and Lefebvre [3], but for lower temperatures we find a weaker solubility in bulk samples as compared to the thin-film solutions of Kovalenko et al. [4]. A noticeable change of the mutual solubility in the Kr–Xe system was found to occur in the close vicinity of the critical point (Fig. 2). By comparing Figs. 2 and 4, the variation of the lattice parameters and the molar volumes with temperature and concentration along the separation curve fairly correlates with the $T-x$ diagram, which is an extra evidence of the critical separation of these mixtures. Numeric values for the molar volumes of the Ar–Xe and Kr–Xe mixtures in

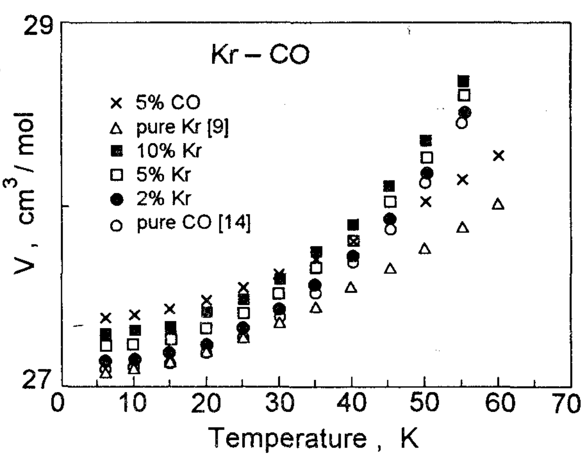

Fig. 5. Temperature dependence of the molar volume of Kr–CO solutions.

the single-phase regions are summarized in Tables 1 and 2.

Table 1

Temperature and concentration dependence of the molar volume of argon - xenon mixtures (in cm^3/mol)

T, K	Ar, mol.%				
	0.0[a]	0.0[b]	5.0[c]	97.5[c]	100.0[d]
6	34.72	—	34.82	22.69	22.557
10	34.73	—	34.83	22.70	22.567
15	34.75	—	34.85	22.73	22.571
20	34.79	—	34.89	22.78	22.643
25	34.85	—	34.96	22.85	22.715
30	34.93	—	35.05	22.94	22.804
35	35.01	—	35.14	23.04	22.909
40	35.10	—	35.24	23.16	23.026
45	35.20	—	35.34	23.29	23.154
50	35.30	—	35.45	23.43	23.295
55	35.41	—	35.56	23.58	23.447
60	35.53	—	35.67	23.75	23.612
65	35.66	—	35.79	23.93	23.790
70	35.79	—	35.91	24.12	23.985
75	35.93	—	36.03	24.33	24.198
78.17	—	35.94	—	—	—
80			36.16	24.57	24.434
83	—	—	—	—	23.588
85.10	—	36.15			

[a] Sears and Klug [8]; [b] Granfors et al. [10]; [c] this work; [d] Peterson et al. [11].

Table 2

Molar volumes of the Kr–Xe solid solutions at various temperatures and Kr concentrations (in cm^3/mol)

T, K	100% Xe[a]	x, % Kr		
		5[b]	97.5[b]	100[c]
6	34.72	34.37	27.44	27.10
10	34.73	34.38	27.46	27.11
15	34.75	34.42	27.49	27.14
20	34.79	34.47	27.55	27.20
25	34.85	34.54	27.62	27.27
30	34.93	34.62	27.71	27.36
35	35.01	34.71	27.82	27.45
40	35.10	34.80	27.93	27.55
45	35.19	34.89	28.04	27.66
50	35.30	34.98	28.15	27.77
55	35.41	35.08	28.27	27.89
60	35.53	35.18	28.39	28.01
65	35.66	35.29	28.52	28.14
70	35.79	35.40	28.66	28.28
75	35.93	35.51	28.81	28.42

[a] Sears and Klug [8]; [b] this work; [c] Losee and Simmons [9].

In contrast to the binary systems of the rare gases, the phase diagram of the Kr–CO system (Fig. 3) is more complex in form, and, besides the critical point, exhibits peritectic, monotectoid, and eutectic points of three-phase equilibrium. This is due to the rotation subsystem of the molecular component present in the given solutions. As the temperature is lowered, the quadrupole-quadrupole interaction in pure CO drives a polymorphic transformation from the high-temperature disordered β-phase of symmetry $P6_3/mmc$ to the ordered α-phase of symmetry $Pa3$ [1]. The phases β_1 and β_2 in the solutions (Fig. 3) are isostructural (hcp) and differ in the degree of hindrance of the rotational state of the CO molecules; this difference vanishes at the critical point. Our diagram of Fig. 3 resembles the ones previously constructed by us for the N_2–Ar [12] and Ar–CO [13] systems with the distinction that the domain of the isostructural β-phases is much narrower in concentration. Effect of impurities on the molar volumes of Kr–CO solid mixtures are quantitatively illustrated in Fig. 5 and Table 3.

Table 3

Molar volumes of the Kr–CO solid solutions at various temperatures and Kr concentrations (in cm^3/mol)

T, K	100% CO [14]	x, % Kr					
		2	3	5	10	95	100 [9]
6	27.11	27.15	27.17	27.23	27.30	27.39	27.10
10	27.11	27.16	27.18	27.24	27.32	27.41	27.11
15	27.16	27.19	27.22	27.27	27.35	27.44	27.14
20	27.19	27.24	27.27	27.33	27.42	27.48	27.20
25	27.28	27.33	27.36	27.41	27.49	27.55	27.27
30	27.39	27.44	27.46	27.52	27.60	27.62	27.36
35	27.52	27.57	27.60	27.66	27.74	27.71	27.45
40	27.69	27.73	27.76	27.82	27.90	27.82	27.55
45	27.89	27.93	27.97	28.02	28.11	27.91	27.66
50	28.13	28.18	28.21	28.27	28.36	28.03	27.77
55	28.45	28.51	28.55	28.60	28.68	28.15	27.89
60		—	—	—	—	28.28	28.01
70	—	—	—	—	—	28.55	28.28
80	—	—	—	—	—	28.84	28.57
90	—	—	—	—	—	29.16	28.88
100	—	—	—	—	—	29.52	29.25

Two facts are noteworthy here. First, in spite of the coincidence of the molar volumes at low temperatures of pure krypton and carbon monoxide, dissolution of the molecular impurity of carbon monoxide in the krypton matrix as well as of krypton atoms in the α-lattice of carbon monoxide entails an increase of the volume of solid solutions. This is evidence that the host-guest interaction differs substantially as compared to the intra-matrix interaction. Second, the molecular impurity affects much stronger the lattice of the atomic crystal as compared to the atomic impurity in the molecular crystal. At equal concentrations of impurities, the excess volume per impurity is larger in the former case by a factor of 3.

In conclusion we shall discuss a fundamental question that arises from results of this work. All the binary alloys of cryocrystals exhibit at low temperature a restricted solubility of the initial components, notwithstanding the fact that the difference of the atomic (molecular) radii does not exceed 15%. This is in shear contradiction with the Hume-Rosery rules [2], which are usually fairly consistent for solid solutions of various metals. Even in such a system as Ar–Kr, where the difference in atomic radii amounts to 6%, cluster formation can be observed [15] within a certain concentration range, which is evidence of inhomogeneity of these solutions and of a precursor of their separation. Thus, we may conclude that, unlike in the metal systems, in binary alloys of cryocrystals the solubility-restricting mechanism is of different physical nature.

The autors are deeply indepted to A. P. Brodyanskii and M. A. Strzhemechny for a fruitful discussion of the results.

1. *Cryocrystals*, B. I. Verkin and A. F. Prikhotko (eds.), Naukova Dumka, Kiev (1983).
2. T. B. Massalski, *Structure of Solid Solutions*, in: *Physical Metallurgy*, R. W. Cahn (ed.), Noth-Holland Publishing Company, Amsterdam (1965).
3. R. Heastie and C. Lefebvre, *Proc. Phys. Soc.* **76**, 180 (1960).
4. S. I. Kovalenko, E. I. Indan, and A. A. Khudoteplaya, *Phys. Status Solidi* **A13**, 235 (1972).
5. R. Heastie, *Physica* **24**, suppl., 182 (1958).
6. M. P. Freeman and G. D. Halsey, *J. Phys. Chem.* **60**, 1119 (1956).
7. S. I. Kovalenko, E. I. Indan, A. A. Khudoteplaya, and I. N. Krupskii, *Phys. Status Solidi* **A24**, 481 (1974).
8. D. R. Sears and H. P. Klug, *J. Chem. Phys.* **37**, 3006 (1962).
9. D. L. Losee and R. O. Simmons, *Phys. Rev.* **172**, 944 (1968).
10. P. R. Granfors, A. T. Macrander, and R. O. Simmons, *Phys. Rev.* **B24**, 4753 (1981).
11. O. G. Peterson, D. N. Batchelder, and R. O. Simmons, *Phys Rev.* **150**, 703 (1966).
12. L. D. Yantsevich, A. I. Prokhvatilov, I. N. Krupskii, and A. S. Barylnik, *Fiz. Nizk. Temp.* **12**, 300 (1986) [*Sov. J. Low Temp. Phys.* **12**, 170 (1986)].
13. A. I. Prokhvatilov and L. D. Yantsevich, *Fiz. Nizk. Temp.* **12**, 882 (1986) [*Sov. J. Low Temp. Phys.* **12**, 502 (1986)].
14. I. N. Krupskii, A. I. Prokhvatilov, A. I. Erenburg, and L. D. Yantsevich, *Phys. Status Solidi* **A19**, 519 (1973).
15. H. M. Gilder, *Phys. Rev. Lett.* **61**, 2233 (1988).